Expanded View Figures

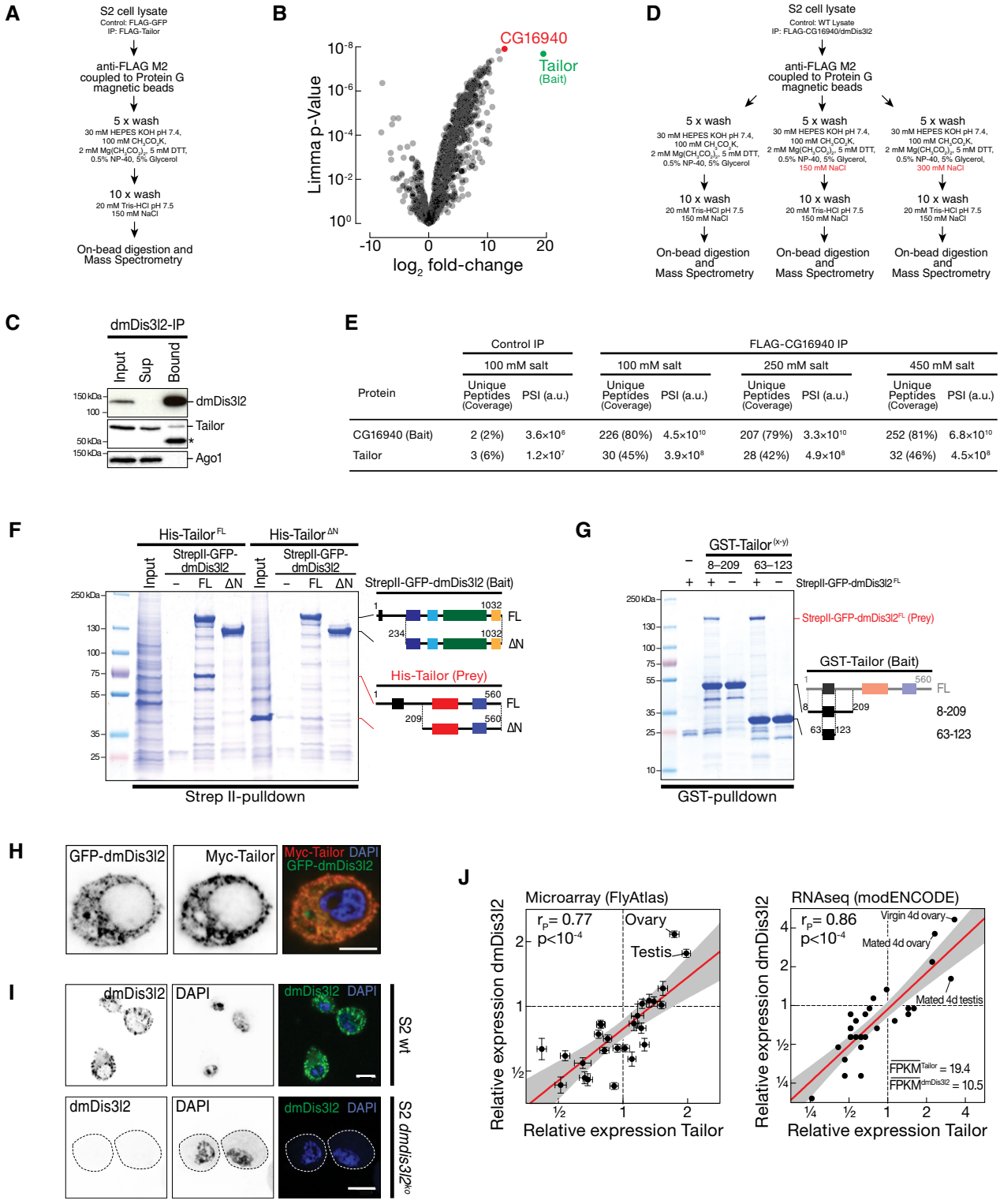

Protein	Control IP 100 mM salt Unique Peptides (Coverage)	Control IP 100 mM salt PSI (a.u.)	FLAG-CG16940 IP 100 mM salt Unique Peptides (Coverage)	FLAG-CG16940 IP 100 mM salt PSI (a.u.)	FLAG-CG16940 IP 250 mM salt Unique Peptides (Coverage)	FLAG-CG16940 IP 250 mM salt PSI (a.u.)	FLAG-CG16940 IP 450 mM salt Unique Peptides (Coverage)	FLAG-CG16940 IP 450 mM salt PSI (a.u.)
CG16940 (Bait)	2 (2%)	3.6×10^{6}	226 (80%)	4.5×10^{10}	207 (79%)	3.3×10^{10}	252 (81%)	6.8×10^{10}
Tailor	3 (6%)	1.2×10^{7}	30 (45%)	3.9×10^{8}	28 (42%)	4.9×10^{8}	32 (46%)	4.5×10^{8}

Figure EV1.

Figure EV1. Identification of the terminal RNA uridylation-mediated processing (TRUMP) complex.

A Experimental overview of FLAG-Tailor co-immunoprecipitation followed by mass spectrometry.
B Limma analysis of protein interaction candidates based on three biological replicates of experiment shown in (A). Tailor (bait) is indicated in green. The most prominent interaction candidate showing highest and significant signal accumulation (CG16940) is shown in red.
C Co-immunoprecipitation of endogenous dmDis3l2 and Tailor. dmDis3l2 was immunoprecipitated from S2 cell lysate using an antibody against endogenous dmDis3l2, followed by Western blot analysis of dmDis3l2 and Tailor. Ago1 serves as a control. Asterisk indicates antibody heavy chain signal.
D Experimental overview of immunopurification using FLAG-CG16940 as bait and applying increasing salt concentrations in wash steps, followed by mass spectrometry analysis.
E Mass spectrometry analysis of the experiment shown in (D). High coverage and signal intensities of Tailor were recovered in FLAG-CG16940 IP, but not in control IP, irrespective of wash conditions.
F, G Recombinant protein interaction studies using the indicated epitope tags and purification methods. Domain architecture of bait and prey are indicated.
H, I Immunostaining and imaging of Myc-Tailor and GFP-dmDis3l2 (H) or endogenous dmDis3l2 (I) in S2 cells (H and I top panel) or S2 cells depleted of dmDis3l2 by CRISPR/Cas9 (I bottom panel). Single-color channel images show total inversions. Scale bar = 5 μm.
J Relative mRNA expression levels of dmDis3l2 and Tailor in different tissues of flies. Analysis is based on published microarray data (FlyAtlas; Chintapalli *et al*, 2007) or RNA-Seq data (ModENCODE; Brown *et al*, 2014).

Source data are available online for this figure.

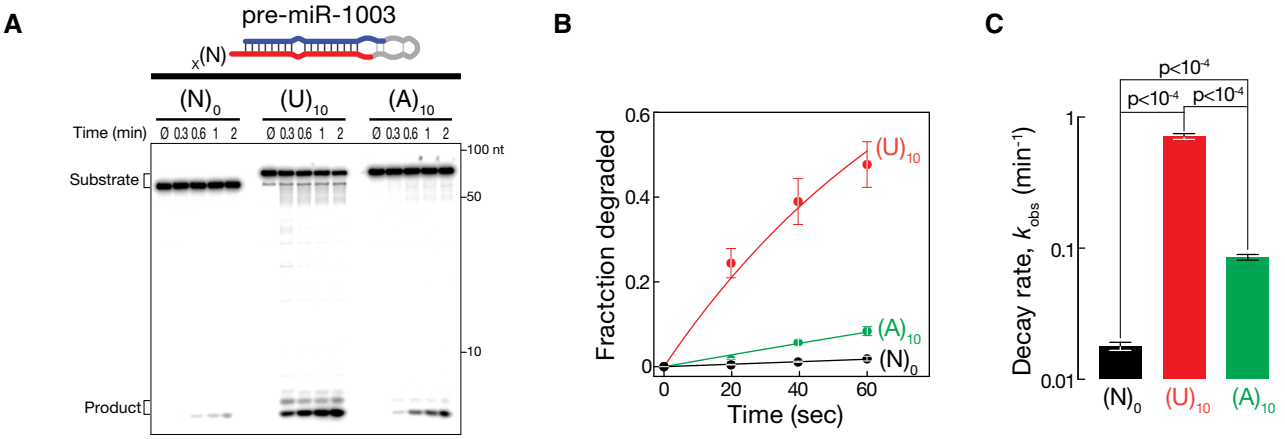

Figure EV2. Uridylation-triggered RNA decay of mirtron hairpins by Tailor and dmDis3l2 *in vitro*.

A RNA decay assay using synthetic, 5′ radiolabeled pre-miR-1003 containing the indicated number of nucleotide extensions, and immunopurified dmDis3l2.
B Quantification of three independent replicates of experiment shown in (A). Data represent mean ± SD. Data were fit to single-exponential decay kinetics.
C Decay rates (k_{obs}) determined in (B). Error bars indicate SEM of fit. *P*-values were determined using Student's *t*-test.

Source data are available online for this figure.

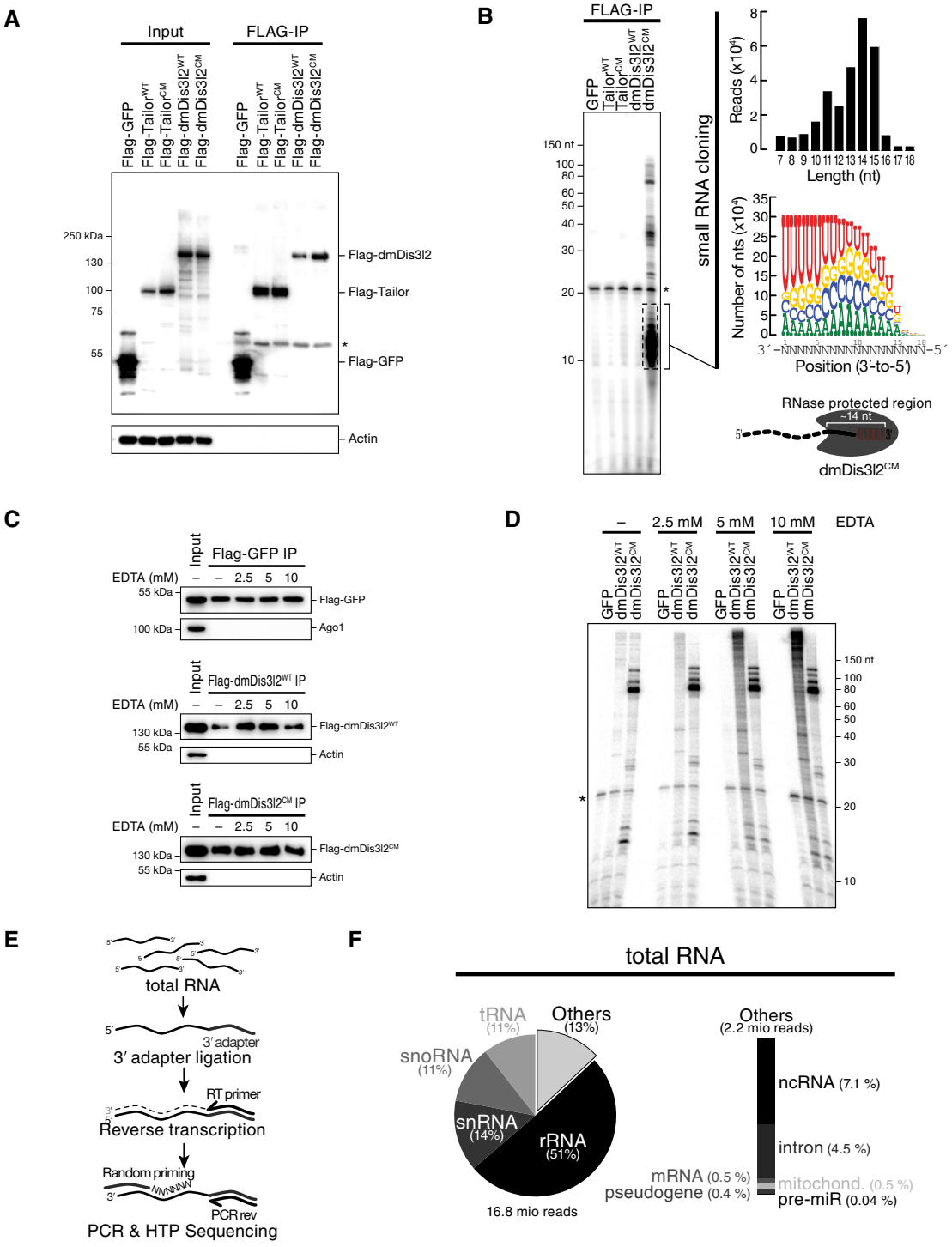

Figure EV3.

Figure EV3. Identification of TRUMP complex substrates by RNA immunoprecipitation and high-throughput sequencing.

A Western blot analysis associated with experiment shown in Fig 5A. Actin serves as a control. Asterisk indicates non-specific signal, corresponding to hc-antibody signal.

B Small RNA sequencing analysis. Strong RNA signal intensities between 10 and 20 nt observed for immunopurified dmDis3l2^{CM} were gel-purified and subjected to small RNA cloning (see Materials and Methods). Resulting libraries were analyzed for RNA length (top right graph) and nucleotide content (bottom right graph). Small RNAs bound to dmDis3l2CM correspond to 3′ uridine-rich, RNase-protected fragments.

C Western blot analysis of FLAG immunopurification in the presence of the indicated concentration of EDTA. Ago1 and actin are controls.

D RNA–protein co-immunopurification experiments in the presence of the indicated concentration of EDTA. FLAG-tagged versions of indicated proteins were expressed in S2 cells, followed by immunopurification and RNA isolation. Co-immunopurified RNA was visualized by CIP/PNK treatment using γ-^{32}P-ATP followed by denaturing polyacrylamide gel electrophoresis and phosphorimaging. Asterisk indicates non-specific contaminant.

E Overview of experimental approach for S2 cell total RNA 3′ end sequencing.

F Statistics of total RNA 3′ end sequencing library generated from S2 cell total RNA following the approach described in (E). rRNA, ribosomal RNA; ncRNA, non-coding RNA; tRNA, transfer RNA; snRNA, small nuclear RNA; snoRNA, small nucleolar RNA; mRNA, messenger RNA; mitochond., mitochondrial RNA; pre-miRNA, precursor microRNA.

Source data are available online for this figure.

Figure EV4. Validation of dmDis3l2CM-bound RNA reveals unprocessed RNA pol III transcripts as targets for TRUMP-mediated decay.

A Northern hybridization experiments using total RNA derived from wild-type (wt) S2 cells, S2 cells depleted of dmDis3l2 by CRISPR/Cas9 (*dmdis3l2*^{ko}), or S2 cells expressing FLAG-tagged catalytic-mutant dmDis3l2 (dmDis3l2$^{CM\ OE}$). A probe against 5S rRNA was used.

B Western blot analysis of ovary lysate derived from wild-type flies (w^{1118}), flies depleted of Tailor (*tailor*$^{c4/6}$) or dmDis3l2 (*dmdis3l2*$^{-/-}$), and flies in which the endogenous *dmdis3l2* locus was edited by CRISPR/Cas9 to express a catalytic-inactive version of dmDis3l2 (*dmdis3l2*$^{CM/CM}$). Levels of dmDis3l2 and Tailor were determined using monoclonal antibodies. Actin serves as a loading control.

C Schematic representation of the predicted structure of *dmdis3l2/cg16940* gene and RNA transcripts. The location of a 5-bp deletion introduced by CRISPR/Cas9 genome engineering in flies (*dmdis3l2*$^{-/-}$), or a mutation introducing an amino acid exchange (D to A) at the predicted catalytic site of dmDis3l2 is indicated and confirmation by Sanger sequencing of a PCR product prepared from the locus of WT (w^{1118}) flies and flies homozygous for *dmdis3l2*$^{-/-}$ *or dmdis3l2*$^{CM/CM}$ is shown.

D Protein domain organization of wild-type dmDis3l2 and a predicted truncation generated by the frameshift mutation shown in (C), as well as the location of the catalytic mutation, is depicted.

E Northern hybridization experiments using total RNA derived from *Drosophila* S2 cells. Wild-type S2 cells, cells depleted of dmDis3l2 by CRISPR/Cas9 (*dmdis3l2*^{KO}), or cells expressing a catalytic-mutant version of dmDis3l2 (dmDis3l2^{CM}) were used. A probe against RNase MRP RNA was used; ethidium bromide staining serves as a loading control.

F Northern hybridization experiments using total RNA derived from adult whole male flies. Wild-type (w^{1118}) flies, flies depleted of dmDis3l2 by CRISPR/Cas9 (*dmdis3l2*$^{-/-}$), or flies homozygous for a point mutation in the predicted catalytic site of endogenous dmdis3l2 (*dmdis3l2*^{CM}) were used. A probe against RNase MRP RNA was used; ethidium bromide staining serves as a loading control.

G Quantification of four independent biological replicates of experiment shown in (E) and (F). Abundance of RNase MRP RNA in the respective genetic mutant background relative to wild-type samples is reported. Values report mean ± SD. *P*-values were determined by Student's *t*-test.

H 3′ end counts for the indicated locus in the *Drosophila melanogaster* genome, corresponding to RNase MRP RNA, in libraries generated from total RNA or dmDis3l2^{CM}-IP. PM, prefix-matching (i.e., tailed); GM, genome-matching.

I Experimental approach to test 3′ end heterogeneity of RNase MRP RNA. A DNA oligonucleotide was annealed to RNase MRP RNA in total RNA followed by RNase H treatment, resulting in the endonucleolytic cleavage of the transcript. Shortening of the transcript enables to test 3′ end heterogeneity in high-resolution Northern hybridization experiments.

J Northern hybridization experiment using the experimental approach described in (I). Total RNA from S2 cells or adult whole male flies of the indicated genotype were used. Probes against the 5′ (top) or 3′ cleavage product (bottom) were used. Signals corresponding to extended, unprocessed 3′ isoforms of RNase MRP RNA are indicated.

K–M 3′ end counts for the indicated loci in the *Drosophila melanogaster* genome, in libraries generated from total RNA or dmDis3l2^{CM}-IP. SnoRNA:U3:54b (K), snoRNA:18S (L), and snRNA:U6 (M) are shown. PM, prefix-matching (i.e. tailed); GM, genome-matching.

Source data are available online for this figure.

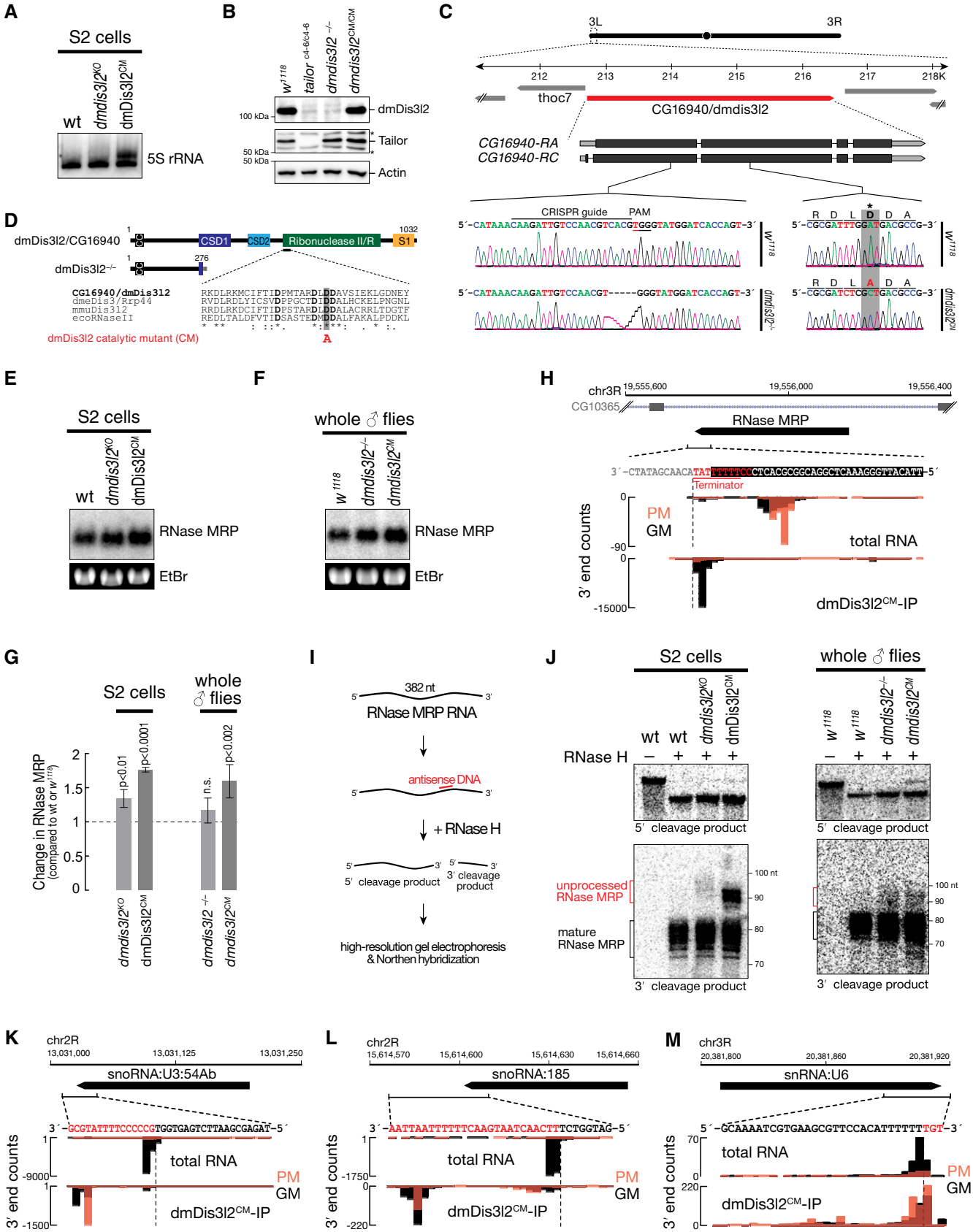
A
S2 cells
wt
dmdis3l2KO
dmDis3l2CM
5S rRNA
B
w1118
tailor c4-6/c4-6
dmdis3l2 −/−
dmdis3l2CM/CM
100 kDa
dmDis3l2
50 kDa
Tailor
50 kDa
Actin
C
3L
3R
212
213
214
215
216
217
218K
thoc7
CG16940/dmdis3l2
CG16940-RA
CG16940-RC
CRISPR guide
PAM
5′-CATAAACAAGATTGTCCAACGTCACGTGGGTATGGATCACCAGT-3′
5′-CATAAACAAGATTGTCCAACGT-----GGGTATGGATCACCAGT-3′
5′-CGCGATTTGGATGACGCCG-3′
5′-CGCGATCTCGCTGACGCCG-3′
w1118
dmdis3l2−/−
dmdis3l2CM
D
dmDis3l2/CG16940
CSD1
CSD2
Ribonuclease II/R
S1
1032
dmDis3l2−/−
276
CG16940/dmDis312
dmeDis3/Rrp44
mmuDis312
ecoRNaseII
RKDLRKMCIFTIDPMTARDLDDAVSIEKLGDNEY
RVDLRDLYICSVDPPGCTDIDDALHCKELPNGNL
RRDLRKDCIFTIDPSTARDLDDALACRRLTDGTF
REDLTALDFVTIDSASTEDMDDALFAKALPDDKL
dmDis3l2 catalytic mutant (CM)
A
E
S2 cells
wt
dmdis3l2KO
dmDis3l2CM
RNase MRP
EtBr
F
whole ♂ flies
w1118
dmdis3l2−/−
dmdis3l2CM
RNase MRP
EtBr
H
chr3R
19,555,600
19,556,000
19,556,400
CG10365
RNase MRP
3′-CTATAGCAACATATTTTTTCCCTCACCCGGCAGGCTCAAAGGGTTACATT-5′
Terminator
3′ end counts
PM
GM
total RNA
dmDis3l2CM-IP
G
S2 cells
whole ♂ flies
Change in RNase MRP (compared to wt or w1118)
p<0.01
p<0.0001
n.s.
p<0.002
dmdis3l2KO
dmDis3l2CM
dmdis3l2 −/−
dmdis3l2CM
I
382 nt
RNase MRP RNA
antisense DNA
+ RNase H
5′ cleavage product
3′ cleavage product
high-resolution gel electrophoresis & Northen hybridization
J
S2 cells
whole ♂ flies
wt
wt
dmdis3l2KO
dmDis3l2CM
w1118
w1118
dmdis3l2−/−
dmdis3l2CM
RNase H
5′ cleavage product
unprocessed RNase MRP
mature RNase MRP
100 nt
90
80
70
3′ cleavage product
K
chr2R
13,031,000
13,031,125
13,031,250
snoRNA:U3:54Ab
3′-GCGTATTTTCCCCCGTGGTGAGTCTTAAGCGAGAT-5′
total RNA
PM
GM
dmDis3l2CM-IP
L
chr2R
15,614,570
15,614,600
15,614,630
15,614,660
snoRNA:185
3′-AATTAATTTTTTCAAGTAATCAACTTTCTGGTAG-5′
total RNA
PM
GM
dmDis3l2CM-IP
M
chr3R
20,381,800
20,381,860
20,381,920
snRNA:U6
5′-GCAAAATCGTGAAGCGTTCCACATTTTTTTGT-3′
total RNA
PM
GM
dmDis3l2CM-IP

Figure EV4.